

CHARACTERIZATION OF SILICON WAFER SURFACES WITH SR-TXRF

P. PIANETTA, A. SINGH, K. LUENING, S. BRENNAN, T. HOMMA¹, N. KUBO¹ AND M. WATANABE²

Stanford Synchrotron Radiation Laboratory, 2575 Sand Hill Rd, Stanford, CA 94309, USA

¹*Waseda University, Dept. of Applied Chemistry, Shinjuku, Tokyo 169-8555, Japan*

²*SEZ, Tokyo, Japan*

Total Reflection X-ray Fluorescence (TXRF) has proven itself to be a valuable tool for non-destructively detecting trace levels of metal contamination on silicon wafer surfaces. Such analyses have become crucial to the semiconductor industry as the levels of metal contamination that can be tolerated in the ultrathin gate dielectrics used in advanced processes have dropped to levels below 10^9 atoms/cm². Furthermore, the implementation of Cu interconnect technology has further complicated the processing environment because of the possibility of cross contamination. This has resulted in a demand for better detection sensitivities together with a need to understand how metals deposit from solution onto the surfaces of the silicon wafers. This paper will describe the advanced capabilities provided by synchrotron radiation TXRF which achieve sensitivities about 50 times better than conventional instruments for transition metals, as well as millimeter scale spatial resolution allowing detailed elemental mapping of the entire wafer surface. In addition, by applying X-ray absorption near edge structure spectroscopy (XANES) in the TXRF geometry, it has been possible to determine the chemical state of atomically dispersed metal atoms and metal nanoparticles intentionally deposited on silicon surfaces from solution.

Introduction

Total reflection X-ray fluorescence in conjunction with synchrotron radiation (SR-TXRF) has demonstrated sensitivities for transition metals that are approximately 50 times better than what is obtained with conventional X-ray sources [1]. With the high flux, low divergence, and linear polarization of a SR source, fluorescence signals are enhanced while background contributions from elastic and inelastic scattering are reduced. Detection limits of 8×10^7 atoms/cm² for transition metals on silicon surfaces have been routinely achieved at the SR-TXRF facility at the Stanford Synchrotron Radiation Laboratory (SSRL) [1]. This has enabled the semiconductor industry to perform high sensitivity surface analyses for process development. The spectrum in Fig. 1 illustrates the best detection limit obtained for Ni of 1.2×10^7 atoms/cm² at SSRL using extended counting times. Given the relatively small footprint of the X-ray beam on the silicon wafer (1 mm \times 7 mm), this detection limit represents a total detected mass of approximately 0.1 fg.

In addition to these "standard" TXRF measurements of metals directly on silicon surfaces, new processes involving Cu interconnect tech-

nologies have created requirements for measuring trace Cu impurities on barrier metals such as Ta. The addition of the heavy metal substrate layer results in a strong Ta L fluorescence signal that overlaps with the Cu K emission line and can even saturate the detector. This problem can be overcome by using the tunability of the SR source to choose an excitation energy below the K edge of Ta yet above that of the Cu. This effectively eliminates the Ta K fluorescence line. However, as we have shown for the analogous case of Al on Si, a significant background is still present due to inelastic X-ray Raman scattering. Generally, the cross-section for X-ray Raman scattering is low compared to the elastic Rayleigh or inelastic Compton scattering, but does become significant due to resonant enhancement if the incident photon energy is close to a major absorption threshold of the sample matrix as is the case here [2, 3]. In spite of this background that can reduce the ultimate sensitivity of the measurement, we will demonstrate below that it is still possible to choose an appropriate photon energy that minimizes these effects and results in a detection limit in the 10^9 atom/cm² range.

While TXRF alone can determine the type and

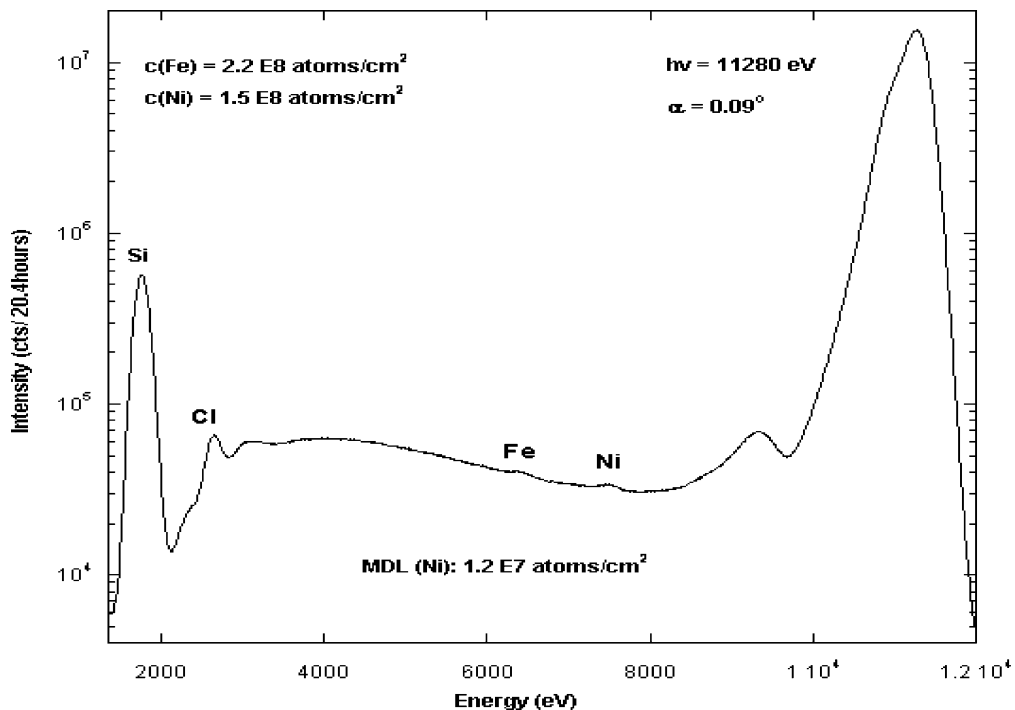
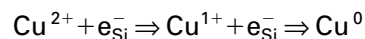


Fig. 1. TXRF spectrum of an unintentionally contaminated wafer taken for 20.4 hours of counting time at an excitation energy of 11.2 keV. The MDL for Ni is 1.2×10^7 atoms/cm². For a standard counting time of 1000 sec, the MDL for Ni is 8×10^7 atoms/cm².

amount of contamination on a silicon wafer surface, chemical state information for each contaminant can be obtained by tuning the excitation energy through the absorption edges of interest and measuring the yield of the relevant fluorescence line as a function of photon energy. The resulting spectrum of the X-ray absorption near edge structure (XANES) provides information on the unoccupied density of states from which the oxidation state of the contaminant can be determined.

One such relevant study involves trace Cu metal deposition onto silicon wafer surfaces from ultra pure water (UPW) solutions that are commonly used by semiconductor manufacturers in post-clean rinse steps. Ever since the implementation of Cu interconnect technology in chip processing, understanding how Cu ions in solution interact with silicon surfaces has been of the utmost importance to the semiconductor industry, particularly since Cu is a fast diffuser in silicon. For metal contamination in solution, there are generally two alternative reaction pathways that depend on the pH value of the solution. In lower pH, i.e., acidic, solutions, it is expected that metal ions are electrochemically reduced and deposited on the surface as metal-

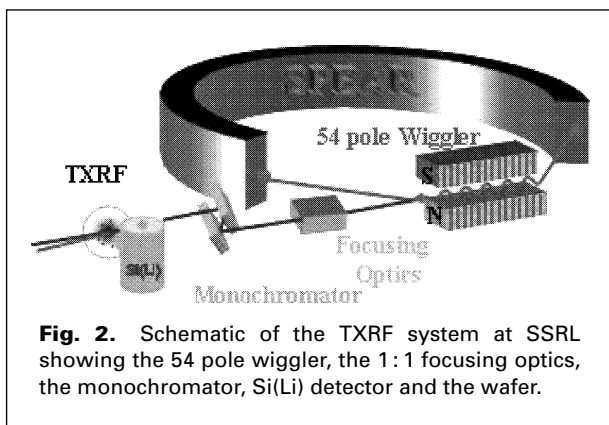
lic particles [4]. For example, Cu metal is reductively deposited on the silicon surface via the following chemical reaction:



Conversely, in higher pH, i.e., basic, solutions, an oxide layer readily forms on the silicon surface, and metal ions are precipitated and included into the oxide layer as a metal oxide/hydroxide [5]. In ultra pure water solutions where the pH is neutral, it is proposed that both reaction pathways can occur simultaneously, and that the deposition mechanism is sensitive to other factors such as the dissolved oxygen content [6]. By utilizing both SR-TXRF and XANES, it is possible to investigate copper deposition mechanisms in UPW solutions [7].

Experiment

The basic experimental configuration used for both the high sensitivity TXRF system and the XANES measurements is shown in Fig. 2 [1]. The source of the radiation used in these experiments is a high flux, 54 pole wiggler on the SPEAR storage ring at the Stanford Synchrotron Radiation Laboratory (SSRL). The beam is focused in a 1:1 geometry onto the sample by a



platinum coated bent cylindrical mirror with a critical energy of 21 keV. For the highest sensitivity studies, the beam is monochromated by a double multilayer monochromator mounted on a standard, water-cooled, two-crystal SSRL monochromator. The multilayers were purchased commercially [8] and consist of alternating layers of Mo and B₄C with a *d*-spacing of 29 Å. The tuning range of the multilayer monochromator is typically set to be from 6 to 14 keV with 11.2 keV being the standard energy for transition metal analysis. This photon energy was chosen because it gives a high cross section for the transition elements while preventing overlap of the detector escape peak with the signals of interest. Higher photon energies are used to excite heavier elements such as As whereas lower photon energies are used eliminate the fluorescence from thin films such as Cu or Ta when they are present on a wafer, in order to avoid detector saturation. The flux transmitted through this optical system is approximately 3×10^{15} photons/sec cm². The monochromator on the TXRF system has been recently upgraded to a liquid nitrogen (LN) cooled system [9] designed to operate under the much higher powers that will be provided by the SSRL's upcoming SPEAR3 upgrade [10, 11]. The improved cooling achieved with this monochromator has eliminated distortions in the monochromator crystals so that a much better focus is achieved at the sample relative to the water-cooled multilayer monochromator. Because of this improved beam focus the overall flux in the analyzed area using the LN cooled Si(111) crystals is only a factor of 10 less than the multilayer system. This improvement has enabled us to obtain XANES spectra of Cu at coverages below the 10^{10} atom/cm² range. In the work described below, all the XANES spectra have been taken with the LN cooled monochromator.

After monochromatization, the beam is shaped by a 0.2 mm × 2 mm entrance slit, and enters the chamber through a Be window and strikes the wafer surface. The wafer is held vertically on an electrostatic chuck mounted on a computer controlled XY stage that allows 150 and 200 mm wafers to be mapped in the beam. Note, that the spatially well defined SR beam enables mapping to the wafer edge with a spatial resolution of about 1 mm in the vertical direction. In addition, software is available to allow localized contamination to be carefully mapped. The wafer is mounted with its surface normal parallel to the polarization vector of the synchrotron radiation. This allows the detector to be mounted both close to the wafer for an increased solid angle and with its axis along the polarization vector minimizing the scattered radiation into the detector. The detector used for these experiments is an energy dispersive Si(Li) solid state detector from Kevex with an 8 μm thick Be window, a 50 mm² active area and an intrinsic resolution of 150 eV for Mn Kα. In addition, the counting rate load on the detector from the Si substrate signal is reduced by a factor of 0.003 by a 25 μm Teflon film that is mounted on the detector. It should also be mentioned that the detector has undergone extensive modifications to eliminate all spurious transition element peaks [12, 13].

The stainless steel vacuum chamber is operated at a pressure of less than 1×10^{-4} Torr in order to eliminate both air scatter and Ar fluorescence. Extreme care has been taken in the design and construction of the chamber as well as the wafer loading, pumping and venting procedures, which are all under computer control, to minimize the possibility of contamination of the sample wafers. In addition, an ULPA filtered mini-environment surrounds the chamber and a robot is used to load and unload the wafers. With these arrangements, it is possible to perform routine wafer analyses with the assurance that no metals will be added to the wafer surface as a result of the measurement.

The orientation of the chamber, wafer and detector are rigidly fixed with respect to each other. In order to vary the angle of incidence of the wafer to the beam, the entire chamber is rotated on a large precision turntable driven by a motorized micrometer. The angle of incidence is determined automatically by fitting the measured reflectivity of the wafer as a function of angle to a theoretical model. Since the quality of the quantification is dependent on accurately controlling the angle of incidence, this measure-

ment is critical and is performed at every point to be measured during a wafer scan. This approach has proven to be extremely reliable and allows for automated mapping of the wafer with reliable quantification. Quantification is achieved by comparing the samples of interest with calibration standards. In the transition metal experiments, the standards used are wafers intentionally contaminated by spin coating with 1×10^{11} atoms/cm² of Fe, Ni and Zn [13]. In addition, wafers prepared with state of the art cleaning processes showing no detectable contamination are used to ensure the absence of parasitic signals as well as measurement induced contamination problems [12].

Applications of SR-TXRF

Wafer Edge Analysis:

Fig. 3 shows typical fluorescence spectra of a wafer, which has been cleaned by a spin process tool of SEZ (SEZ RST201). First the wafer was coated with a Ta barrier layer and a subsequent Cu layer, which was then removed by HNO₃ from the front side followed by a spin cleaning for 6 minutes. The remaining Cu impurity distribution was mapped with special emphasis to the wafer edge, in order to investigate the capability to effectively remove Cu by this particular spin-cleaning process. The top spectrum in Fig. 3 shows a typical fluorescence spectrum measured at the center of the 200 mm wafer, the second spectrum at 50 mm below the center, the third spectrum at 5 mm from the wafer edge and the following spectra (4–7) in 1 mm distances approaching the wafer edge with the lowest spectrum right at the edge position. All TXRF spectra were collected at an angle of incidence of 0.12° and measured for 250 sec. The individual spectra have been shifted vertically for clarity of presentation. The high energy peak is the signal from the scattered synchrotron radiation at 9100 eV, which is below the Ta L and above the Cu K absorption thresholds resulting in highest detection sensitivities for Cu. Note, this particular photon energy is chosen in order to efficiently excite Cu K fluorescence while suppressing the Ta L fluorescence (*i.e.*, the photon energy is below the Ta L edge at 10.2 keV), which would saturate the detector as well as dominate the spectrum wiping out all other structures in the spectrum. However, for all the spectra, this results in an additional signal at about 7200 eV due to resonant X-ray Raman scattering, which is an inelastic scattering process [2, 3]. Note, that this Raman

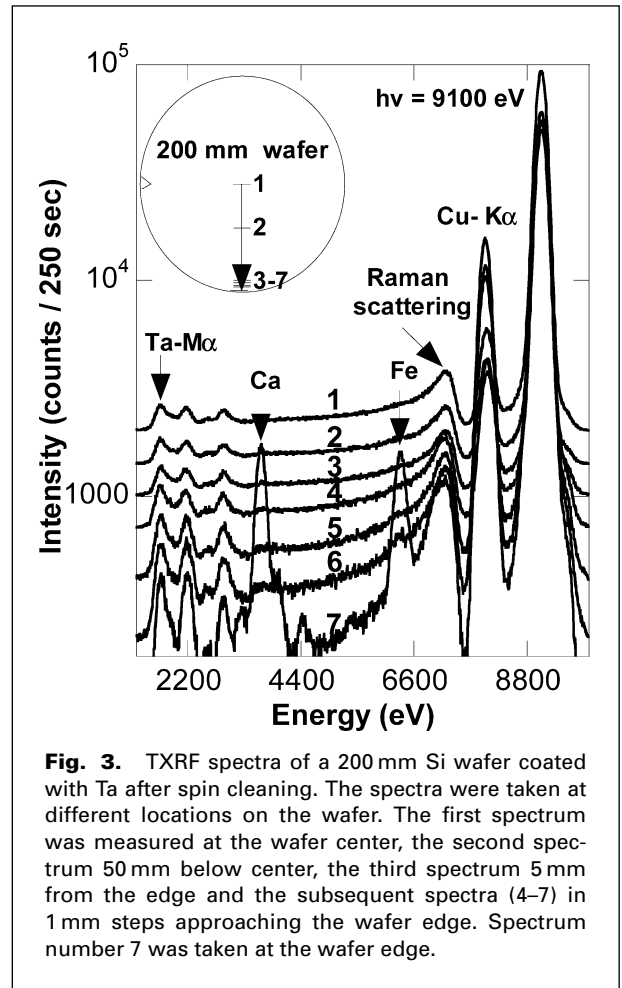


Fig. 3. TXRF spectra of a 200 mm Si wafer coated with Ta after spin cleaning. The spectra were taken at different locations on the wafer. The first spectrum was measured at the wafer center, the second spectrum 50 mm below center, the third spectrum 5 mm from the edge and the subsequent spectra (4–7) in 1 mm steps approaching the wafer edge. Spectrum number 7 was taken at the wafer edge.

structure is not only a single peak but is accompanied by a low energy tail, which creates additional background. This background strongly affects the detection sensitivity for transition metals ranging from Ti up to Ni. However, for this particular excitation energy of 9100 eV, the inelastic Raman scattering does not affect the detection sensitivity for Cu trace impurities, because the fluorescence signature for Cu at 8048 eV is exactly between the scatter and the inelastic Raman peak. This analysis demonstrates that Cu is homogeneously distributed over the whole wafer surface corresponding to about 1×10^{11} atoms/cm². Only the last spectrum taken right at the edge position shows, in addition to Cu, higher impurity levels of Ca as well as Fe. Note that the fluorescence signature in the low energy part of the spectra around 1710 eV is due to Ta M fluorescence and not a signature from the Si substrate.

Chemical State of Cu Trace Impurities on Si
Hydrogen terminated samples were dipped

into a solution of 0.5% HF for 1 minute to prepare a clean, hydrogen terminated surface. In order to study the influence of oxygen, an ultra-pure water (UPW) solution was prepared by Argon sparging (bubbling Ar through the UPW), reducing the dissolved O₂ content to 0.3 ppm, while a non-sparged ultra-pure water solution contains 3.4 ppm of dissolved oxygen. Cu in a 2% nitric acid matrix was then introduced at a concentration level of 100 ppb into the sparged and non-sparged UPW. Surface contamination was then accomplished by immersing the hydrogen terminated silicon samples into these solutions. The samples were then dried with an Ar gas jet and immediately introduced into the TXRF chamber and put under vacuum to prevent oxidation of the deposited Cu atoms. The surface concentrations were measured with TXRF prior to taking the XANES spectra.

The XANES measurements were carried out using the high-resolution, LN-cooled, double-crystal (Si 111) monochromator with an energy resolution of 0.89 eV at 8.9 keV. The excitation energy was tuned through the K edge (8.979 keV) in the grazing incidence TXRF geometry while monitoring the fluorescence yield originating from the decay of the excited core state vacancy. The spectra were obtained between 8.940 and 9.2 keV using the following incre-

ments: 0.5 eV between 8.97 and 8.99 keV near the copper K edge; 1 eV above the edge between 8.99 to 9.060 keV; and 5 eV between 9.06 and 9.2 keV. The signal was integrated for 10 seconds per point for each scan and up to 6 scans were accumulated to achieve a high signal to noise ratio.

In addition, CuO and Cu₂O reference samples, prepared as thin powder samples in a cell with Kapton windows, and a 5 μm thick Cu foil were measured in the transmission geometry using ion chambers placed in front and behind the sample. The absorption coefficient is then obtained according to the Lambert-Beer law [14]:

$$I(d) = I_0 \exp(-\mu \rho d)$$

where I_0 is the incident X-ray intensity, $I(d)$ the intensity after penetration to depth d , ρ is the density of the material, and μ is the mass-absorption coefficient which depends on the energy of the incoming X-rays.

Fig. 4 shows typical TXRF spectra for the silicon samples that had been submerged in 100 ppb copper contaminated UPW solutions. The solid line corresponds to the TXRF spectrum of the wafer dipped into the sparged (=deoxygenated) UPW solution and the dashed line represents the spectrum of a wafer dipped into the non-sparged (=oxygenated) UPW solution.

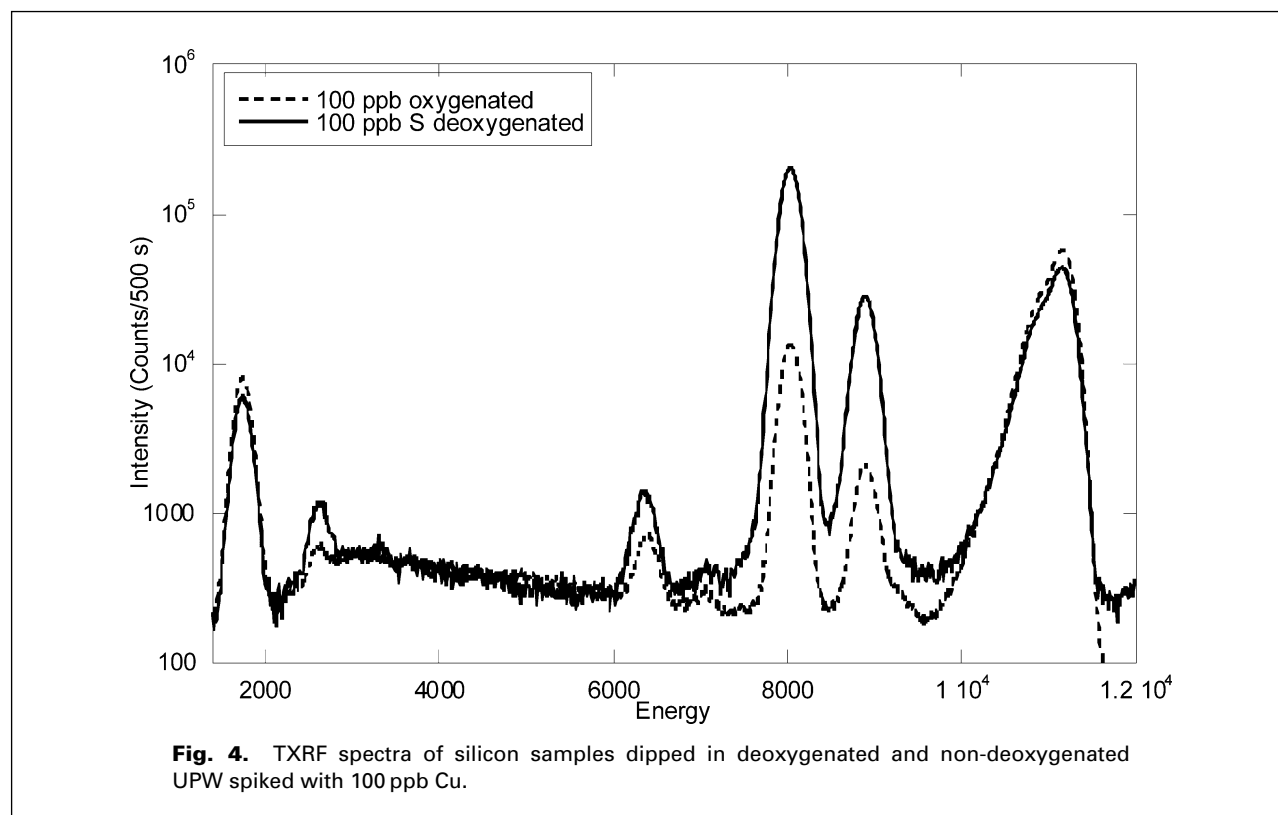


Fig. 4. TXRF spectra of silicon samples dipped in deoxygenated and non-deoxygenated UPW spiked with 100 ppb Cu.

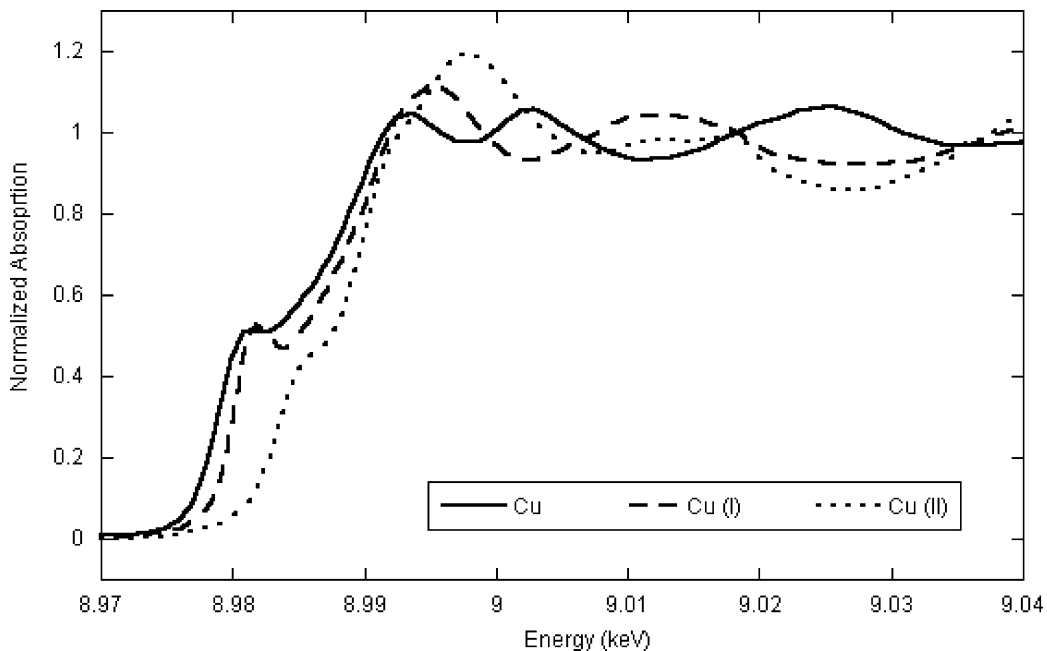


Fig. 5. Cu K XANES spectra taken in transmission for reference samples of Cu, Cu₂O, and CuO. Each of these reference samples represents Cu in a different oxidation state.

Both spectra show the Cu K α and K β fluorescence lines at 8048 and 8905 eV, respectively, from the intentional contamination as well as the Fe K α fluorescence line at 6404 eV due to unintentional Fe contamination at levels below 1×10^9 atoms/cm². It was determined that the Cu concentrations for the 100 ppb sparged and non-sparged samples shown were 2.8×10^{11} and 4.9×10^{12} atoms/cm², respectively.

From the SR-TXRF measurements, it can be seen that there is a factor of 18 increase in the amount of Cu deposited on silicon in a sparged solution as compared to a non-sparged solution. This increase in the amount of deposited copper in a sparged solution can be attributed to the deposition mechanism occurring at the silicon surface. In sparged solutions, it would be expected that the primary mode of Cu deposition would be reductive, resulting in Cu metal cluster formation, while in non-sparged solutions, Cu precipitates into the growing oxide as Cu oxide/hydroxide. However, it has recently been experimentally verified by SR-TXRF measurements, that at low concentrations such as 10 ppb, the concentration in the UPW is not high enough for metal cluster growth in deoxygenated solutions, and any deposited Cu is redissolved by the UPW solution. Therefore, the only Cu that is deposited at 10 ppb occurs by precipitation into the oxide. This results in higher

amounts of deposited Cu for the air saturated solution, since an oxide grows more readily when compared to the deoxygenated solutions. Alternatively, at higher concentrations, such as 100 ppb, Cu cluster growth via the reductive mechanism can occur and therefore the amount of Cu deposited is higher for the de-oxygenated solutions since Cu is deposited both reductively and incorporated into the oxide.

Fig. 5 shows the K edge absorption spectra of the Cu reference samples (Cu, Cu₂O and CuO) having the oxidation state 0, I, and II, respectively. The Cu K edge was determined by the first inflection point, corresponding to 8.979 keV [15], and each spectrum was energy calibrated with respect to a Cu reference metal spectrum that was measured in parallel. A linear background fit to the pre-edge region was subtracted, and each spectrum was normalized with a spline fit done from the post-edge region starting at 9 keV up to 9.2 keV. It can be seen that the Cu K edge shifts to higher binding energies with increasing oxidation state of the Cu sample. In addition to this energy shift, the detailed shape of the structure in the near edge region is strongly dependent on the atomic structure around the absorbing atoms.

Fig. 6 shows the Cu K edge absorption spectra of silicon samples that were contaminated in sparged and non-sparged UPW solutions with

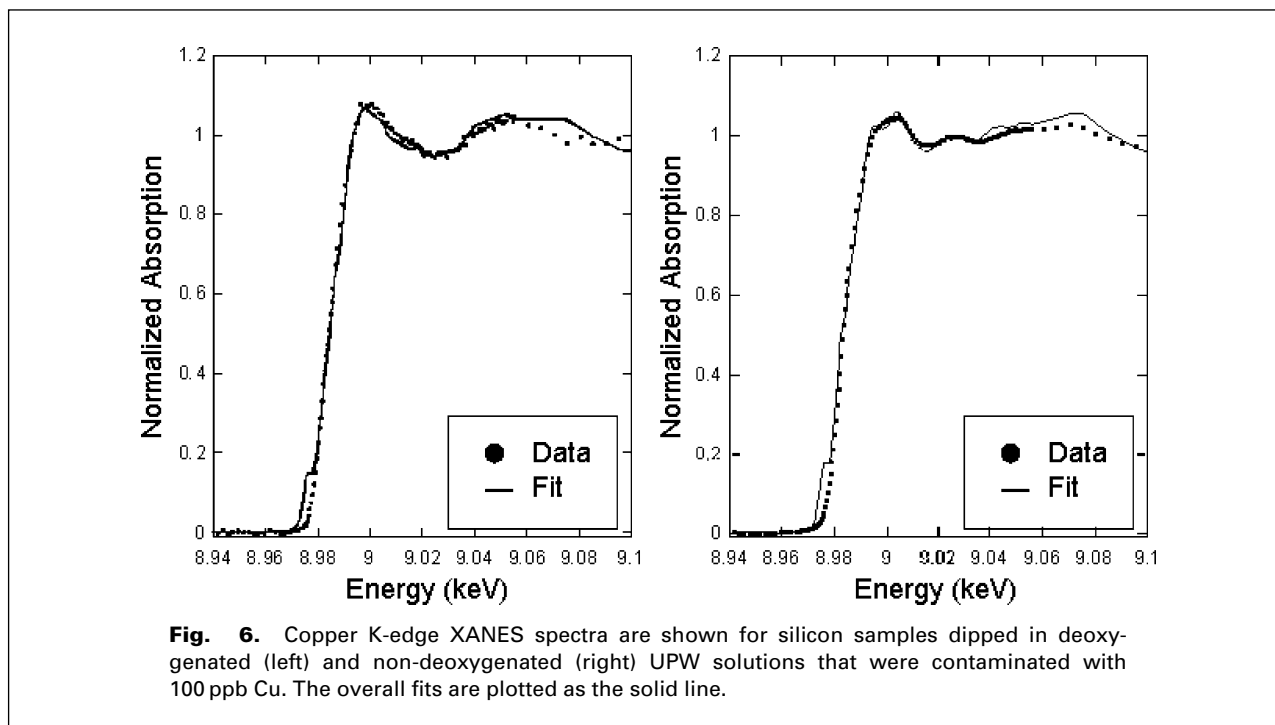


Fig. 6. Copper K-edge XANES spectra are shown for silicon samples dipped in deoxygenated (left) and non-deoxygenated (right) UPW solutions that were contaminated with 100 ppb Cu. The overall fits are plotted as the solid line.

Table 1. Fractional contributions for the XANES fits shown in Fig. 6.

	100 ppb Deoxygenated	100 ppb Oxygenated
Cu metal	.53	.33
Cu (I) Oxide	.30	.27
Cu (II) Oxide	.17	.41

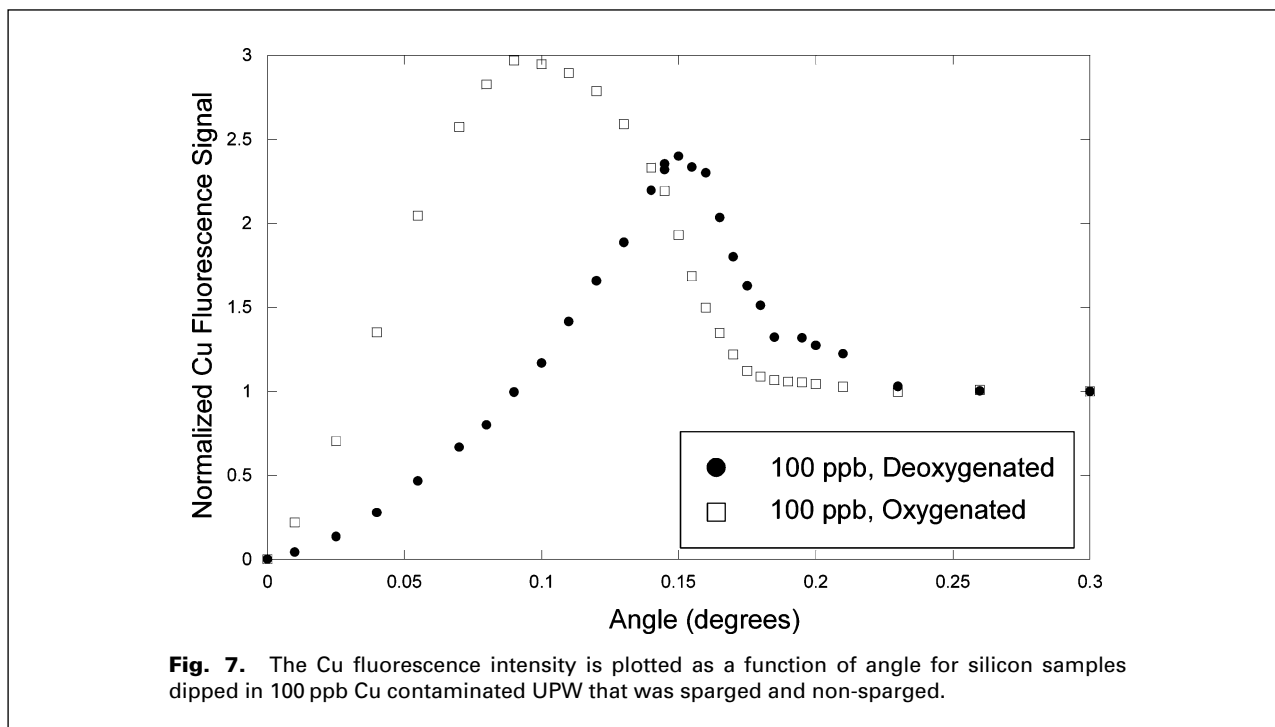
an intentional Cu concentration of 100 ppb. A linear background subtraction and normalization using a spline fit to the post edge region was conducted. Fits were made using linear combinations of the reference XANES spectra of Fig. 5. These fits were conducted from 8.99 to 9.1 keV by performing a chi-squared minimization procedure with the WinXAS program [16] between the XANES data and a linear combination of the reference samples. The numerical results of these fits are shown in Table 1. From these fits of the X-ray absorption spectra it can be seen that the Cu deposited onto the silicon sample surface for the sparged solution with 100 ppb of Cu is mostly metal in character. In contrast, the Cu deposited onto the silicon sample surface for the 100 ppb non-sparged ultra pure water solutions consisted of less Cu metal and more of the Cu oxides. It is proposed that in the absence of dissolved oxygen in ultra pure water solution, copper from solution deposits reductively onto the silicon surface resulting in surface species that is mostly metallic in charac-

ter. On the other hand, the presence of oxygen inhibits reductive deposition and copper species are incorporated into a growing oxide, resulting in surface species that are more oxide in character.

Measurement of Cu Nanoparticle Size by SR-TXRF

By measuring the fluorescence intensity as a function of the incidence angle of the primary X-ray beam and fitting that curve to theoretical model calculations one can precisely determine the size of the Cu nanoparticles deposited on the silicon surface. This is due to the fact that by changing the angle of incidence, the period of the electric field from the standing wave above the silicon surface can be controlled. Therefore, the angular dependence of the fluorescence intensity from a particle with a certain diameter will depend on the integral of the intensity profile over the height of the particle. This results in one or more maxima in fluorescence intensity that occurs before the critical angle for total external reflection. This is in contrast to atomically dispersed species, in which the maximum fluorescence intensity occurs at the critical angle.

In Fig. 7, the Cu fluorescence intensity is plotted as a function of the angle for samples immersed in 100 ppb Cu contaminated UPW. As can be seen, the non-sparged sample has a profile indicative of atomically dispersed Cu, where



the maximum in fluorescence intensity occurs at the critical angle of 0.16 degrees. On the other hand, the sparged sample has a fluorescence maximum at 0.1 degrees suggesting that Cu particles are present on the surface. The preliminary analysis of the angle scans indicates the presence of nanoparticles with a mean diameter of 5–6 nm. These differences in Cu deposition occur because in non-sparged UPW solutions, the growing oxide uses most of the nucleation sites preventing Cu clusters from nucleating. However, in sparged UPW, the oxide grows less slowly allowing for Cu to nucleate mainly as metallic particles.

Conclusion

Synchrotron radiation provides important extensions to laboratory-based TXRF instruments in terms of greatly improved sensitivities, selective excitation of contaminants, higher spatial resolution as well as spectroscopic capabilities. Ultimate sensitivities in the low 10^7 atom/cm² range for transition elements have been demonstrated at the SR-TXRF facility at the Stanford Synchrotron Radiation Laboratory. In addition, by choosing the appropriate photon energy, it is possible to suppress strong substrate fluorescence lines from a high-Z element such as a Ta film in order to observe trace element contamination from adsorbed Cu atoms. Furthermore, XANES performed in the TXRF geometry can be used to determine the oxidation state of trace

contaminants deposited onto silicon surfaces from solution. In the example given for Cu deposition from UPW, it was found that Cu deposited from a deoxygenated UPW solution contaminated with 100 ppb copper was primarily metallic in character while the Cu deposited from a non-deoxygenated UPW solution with the same Cu concentration had Cu in all three oxidation states. In addition, angular scans showed that the metallic copper deposited in the form of nanoparticles with a mean diameter of 5–6 nm.

Acknowledgements

We would like to thank the staff at SSRL for their expert technical assistance. This work was performed at SSRL, which is supported by the Department of Energy, Office of Basic Energy Sciences. The support of SIWEDS is also acknowledged.

References

- [1] P. Pianetta, K. Baur, A. Singh, S. Brennan, J. Kerner, D. Werho, and J. Wang, *Thin Solid Films* **373**, 222 (2000).
- [2] C. J. Sparks, *Phys. Rev. Lett.* **33**, 262 (1974).
- [3] K. Baur, J. Kerner, S. Brennan, A. Singh, P. Pianetta, *J. Appl. Phys.* **88**, 4642, (2000).
- [4] H. Morinaga, M. Suyama and T. Ohmi, *J. Electrochem. Soc.* **141**, 2834 (1994).
- [5] Morinaga, M. Aoki, T. Maeda, M. Fujisue, H. Tanaka and M. Toyoda, *Mat. Res. Soc. Symp. Proc.* **477**, 57 (1997).

- [6] T. Homma and C. Chidsey, *J. Phys. Chem.* **B102**, 7919 (1998).
- [7] A. Singh, K. Baur, S. Brennan, T. Homma, N. Kubo, and P. Pianetta, *Mat. Res. Soc. Symp. Proc.* **716**, 23 (2002).
- [8] Osmic Inc., Troy, MI.
- [9] M. Rowen, J. W. Peck, T. Rabedeau, *Nuc. Inst. and Meth.* **467**, 400 (2001).
- [10] R. Boyce, S. Brennan, J. Corbett, M. Cornacchia, W. Davies-White, A. Garren, R. Hettel, A. Hofmann, C. Limborg, Y. Nosochkov, H.-D. Nuhn, T. Rabedeau, J. Safranek, H. Wiedemann, *Proceedings of the 1997 Particle Accelerator Conference* **1**, 838 (1997).
- [11] J. Corbett, R. Akre, P. Bellomo, R. Boyce, L. Cadapan, R. Cassel, B. Choi, D. Dell'Orco, I. Evans, T. Elioff, R. Fuller, A. Garren, R. Hettel, D. Keeley, N. Kurita, J. Langton, G. Leyh, C. Limborg, D. Macnair, D. Martin, E. Medvedko, C. Ng, Y. Nosochkov, J. Olsen, M. Ortega, C. Pappas, S. Park, T. Rabedeau, H. Rarback, A. Ringwall, P. Rodriguez, J. Safranek, H. Schwarz, B. Scott, J. Sebek, S. Smith, J. Tanabe, A. Terebilo, C. Wermelskirchen, *Proceedings of the 2002 European Particle Accelerator Conference*, 665 (2002).
- [12] N. Takaura, S. Brennan, P. Pianetta, S. S. Laderman, A. Fischer-Colbrie, J. B. Kortright, D. C. Wherry, K. Miyazaki, and A. Shimazaki, *Advances in X-ray Chemical Analysis JAPAN* **26**, 113 (1995).
- [13] Fischer-Colbrie, S. S. Laderman, S. Brennan, S. Ghosh, N. Takaura, P. Pianetta, A. Shimazaki, D. C. Wherry, and S. Barkan, *Mat. Res. Soc. Symp. Proc.* **477**, 403 (1997).
- [14] E. Gullickson in *X-ray Data Booklet* edited by A. Thompson and D. Vaughan (Lawrence Berkeley Labs, Berkeley, 2001), pp. 1–38.
- [15] G. P. Williams in *X-ray Data Booklet* edited by A. Thompson and D. Vaughan (Lawrence Berkeley Labs, Berkeley, 2001), pp. 1–3.
- [16] T. Ressler, *J. Synchrotron Rad.* **5**, 118 (1998).